Biomaterials 140 (2017) 115–127

Contents lists available at ScienceDirect

Biomaterials

journal homepage: www.elsevier.com/locate/biomaterials

A highly adhesive and naturally derived sealant

Alexander Assmann [a, b, c, d], Andrea Vegh [a, b, e], Mohammad Ghasemi-Rad [a, b], Sara Bagherifard [a, b, f], George Cheng [g, h], Ehsan Shirzaei Sani [i], Guillermo U. Ruiz-Esparza [a, b], Iman Noshadi [a, b, c, i], Antonio D. Lassaletta [h], Sidhu Gangadharan [h], Ali Tamayol [a, b, c], Ali Khademhosseini [a, b, c, j, k, **], Nasim Annabi [a, b, c, i, *]

[a] Biomaterials Innovation Research Center, Brigham and Women's Hospital, Harvard Medical School, 65 Landsdowne Street, Cambridge, MA, 02139, USA
[b] Harvard-MIT Division of Health Sciences and Technology, Massachusetts Institute of Technology, Cambridge, MA, 02139, USA
[c] Wyss Institute for Biologically Inspired Engineering, Harvard University, Boston, MA, 02115, USA
[d] Department of Cardiovascular Surgery and Research Group for Experimental Surgery, Heinrich Heine University, Medical Faculty, 40225, Duesseldorf, Germany
[e] Department of Materials Science and Engineering, University of Toronto, Toronto, Ontario, M5S1A4, Canada
[f] Department of Mechanical Engineering, Politecnico di Milano, Milan, 20156, Italy
[g] Division of Pulmonary, Allergy, and Critical Care, Duke University Medical Center, Durham, NC, 27710, USA
[h] Division of Thoracic Surgery and Interventional Pulmonology, Beth Israel Deaconess Medical Center, Boston, MA, 02215, USA
[i] Department of Chemical Engineering, Northeastern University, Boston, MA, 02115-5000, USA
[j] Department of Physics, King Abdulaziz University, Jeddah, 21569, Saudi Arabia
[k] Department of Bioindustrial Technologies, College of Animal Bioscience and Technology, Konkuk University, Hwayang-dong, Gwangjin-gu, Seoul, 05029, Republic of Korea

ARTICLE INFO

Article history:
Received 17 June 2016
Received in revised form
28 May 2017
Accepted 3 June 2017
Available online 6 June 2017

Keywords:
Gelatin methacryloyl (GelMA)
Hydrogel
Lung lesion
Sealant
Wound repair

ABSTRACT

Conventional surgical techniques to seal and repair defects in highly stressed elastic tissues are insufficient. Therefore, this study aimed to engineer an inexpensive, highly adhesive, biocompatible, and biodegradable sealant based on a modified and naturally derived biopolymer, gelatin methacryloyl (GelMA). We tuned the degree of gelatin modification, prepolymer concentration, photoinitiator concentration, and crosslinking conditions to optimize the physical properties and adhesion of the photocrosslinked GelMA sealants. Following ASTM standard tests that target wound closure strength, shear resistance, and burst pressure, GelMA sealant was shown to exhibit adhesive properties that were superior to clinically used fibrin- and poly(ethylene glycol)-based glues. Chronic *in vivo* experiments in small as well as translational large animal models proved GelMA to effectively seal large lung leakages without the need for sutures or staples, presenting improved performance as compared to fibrin glue, poly(ethylene glycol) glue and sutures only. Furthermore, high biocompatibility of GelMA sealant was observed, as evidenced by a low inflammatory host response and fast *in vivo* degradation while allowing for adequate wound healing at the same time. Combining these results with the low costs, ease of synthesis and application of the material, GelMA sealant is envisioned to be commercialized not only as a sealant to stop air leakages, but also as a biocompatible and biodegradable hydrogel to support lung tissue regeneration.

1. Introduction

While traditional surgical closure and treatment of tissue defects is achieved by sutures, staples, or wires, the application of adhesives for different types of lesions is essential. The repair of parenchymatous defects, such as in the lungs, liver, or kidney, is particularly challenging since the consistency of these tissues does

* Corresponding author. Department of Chemical Engineering, Northeastern University, Boston, MA, 02115-5000, USA.
** Corresponding author. Biomaterials Innovation Research Center, Brigham and Women's Hospital, Harvard Medical School, 65 Landsdowne Street, Cambridge, MA, 02139, USA.
E-mail addresses: alik@bwh.harvard.edu (A. Khademhosseini), n.annabi@neu.edu (N. Annabi).

http://dx.doi.org/10.1016/j.biomaterials.2017.06.004
0142-9612/

not facilitate strong fastening of sutures or staples. Within the lungs, repetitive and quickly varying stress exerted by respiration poses additional risks for failure of the repaired tissue, which is further complicated by the non-sterile environment in the pulmonary airways, creating the possibility of wound infection [1]. Even in tissues that can be sutured, the usage of adhesives may be necessary to allow for better sealing, such as in the closure of small stitching channels in a sutured artery wall [2]. Furthermore, limited access to defect sites can make conventional suturing nearly impossible since there is often not enough space to place sutures. This issue may be solved by applying adhesive prepolymers that polymerize on site, since these materials can be delivered to the area of interest through thin applicators [3,4].

For maximum clinical efficacy, tissue adhesives must demonstrate strong adhesiveness to the tissue, not only to initially close the defect, but to also allow for subsequent wound healing. During this process, controlled degradation of the applied adhesive is desirable [5]. The adhesive should also be biocompatible to avoid an excessive host inflammatory response [6]. Furthermore, most clinical applications require an adhesive with the ability to function under wet conditions. Economic aspects to be considered include application and curing within a reasonable period of time as well as cheap and safe production of the material [7]. Besides these requirements, further features may be desirable depending on the target tissues. For example, defects in highly vascularized tissues require adhesives with hemostatic properties, air or liquid leakages necessitate effective sealants that withstand high pressures, and lesions in flexible tissues should be treated with elastic adhesives to preserve their functionality. Thus, it is crucial to optimize the adhesion and physical properties of tissue adhesives based on the desired applications.

Various types of surgical adhesives and sealants that are comprised of natural, synthetic, and semi-synthetic substances have previously been developed [8,9]. The most common naturally derived tissue adhesives are fibrin- and collagen-based adhesives. While these adhesives are biocompatible, their major drawbacks are their low mechanical characteristics and adhesion strength as well as high production costs and risk of infectious contamination, resulting from the biological source of the materials [10,11]. On the other hand, synthetic-based adhesives, especially clinically used cyanoacrylates, exhibit improved adhesion strength as compared to naturally derived sealants. However, they also provide low biocompatibility and biodegradability, and evoke a foreign body response or even necrosis due to toxic degradation products. Moreover, due to their high stiffness, cyanoacrylate-based adhesives impede physiological movement of elastic and soft tissues such as in the lungs, heart, and blood vessels. Due to these limitations, their usage is predominantly limited to external applications such as the closure of skin wounds [10,11].

The adherence of most tissue adhesives is restricted to dry tissue surfaces. Polymeric hydrogel-based sealants/adhesives can crosslink even under wet conditions and can serve as fluid barriers [12]. Predominantly, poly(ethylene glycol) (PEG)-based formulations such as Coseal™, DuraSeal™ and FocalSeal® have been tested as adhesives both *in vitro* and *in vivo* [13–18]. Unmodified PEG is non-immunogenic, which favors its *in vivo* applications, whereas its inert properties also avoid ingrowth of cells and do not allow tissue healing and repair [16]. Furthermore, due to low mechanical and adhesive characteristics of commercially available hydrogel-based sealants, their clinical indications are predominantly focused on the additional sealing of sutures, and not on the use in suture-free surgical procedures [18,19].

Highly elastic hydrogel-based sealants have been developed for the sealing and closure of elastic tissues such as the lungs. However, most of these sealants lack the appropriate mechanical properties, adhesion strength, and burst pressure performance required for sealing of lung tissue leakages [4]. Adequate lung leakage repair requires sealants with high elasticity that feature strong mechanical and adhesive characteristics even under repetitive and extensive tension. After lung surgery, a prolonged air leak is one of the most common complications, leading to extended chest tube drainage time, which is associated with pain and immobilization for the patient. This in turn increases the risk of infections and broncho-pleural fistulae and, subsequently, leads to a longer hospital stay with associated higher healthcare costs [20–23]. In order to prevent these complications, a variety of natural and synthetic materials have been examined for use, including fibrin sealants, collagen-based sealants, and synthetic glues [24]. For example, a photopolymerizable gelatin-based lung sealant has been developed by covalently crosslinking di-tyrosine in gelation in the presence of ruthenium and sodium persulphate (SPS) [25]. The engineered sealants exhibited a lap adhesion strength higher than commercially available adhesives, like fibrin-based products, and induced minor inflammation at the sealed site in the lungs after 2 weeks. Although the optimized sealant formulation was highly elastic with an extensibility of up to 650%, its low elastic modulus (14 kPa) may not provide suitable cohesive properties for lung sealing. In addition, the high concentrations of SPS (20 mM) and porcine gelatin (17.5%) used to obtain this highly elastic gelatin hydrogel induced toxicity in the *in vitro* studies. Progel™ (Neomend, Irvine, CA, USA), based on human albumin and a PEG crosslinker, has been commercialized as the flagship sealant product to stop air leakage in lung procedures and has shown good burst pressure results [26,27]. However, the high cost of isolating human albumin and the potential for disease transmission causes concerns, as it does for other blood-derived products. Another limitation of Progel™ is that, as a product based on albumin and PEG, it lacks the function of hemostasis, which may be required for sealing when there is blood emanating from the wound. In summary, due to the above-mentioned limitations of lung adhesives/sealants, the introduction of a new biocompatible, highly adhesive, and elastic sealant with strong mechanical properties is warranted.

Photopolymerization of gelatin methacryloyl (GelMA) is an inexpensive and technically simple approach to fabricate hydrogels for biomedical applications [28–33]. The cytocompatibility of GelMA hydrogel has been previously proven *in vitro* and *in vivo*, implying its potential to be used as a suitable biomaterial for various tissue engineering applications [34–36]. While the engineered formulation of GelMA hydrogel was suitable for 3D cell spreading and engineering vascularized tissues, this particular composition did not provide adequate adhesion to wet surfaces to allow for usage as a flexible and highly adhesive sealant.

The present study is aimed at engineering an optimized formulation of GelMA hydrogels to act as tissue adhesives and sealants for the closure of defects in highly stressed elastic tissues such as the lungs. To obtain a GelMA sealant with high adhesion strength, the degree of gelatin modification, the prepolymer concentration, the photoinitiator concentration, and the crosslinking conditions of GelMA prepolymers were optimized. Different ASTM (American Society for Testing and Materials) standard tests were followed to characterize and optimize the adhesive properties of the GelMA sealant, which were compared to several clinically available fibrin- and PEG-based glues/sealants. Furthermore, the biocompatibility of the engineered GelMA sealant was tested using a rat subcutaneous implantation model. The *in vivo* performance of the engineered material for sealing lung leakages was also evaluated using chronic rat and porcine lung incision models.

2. Materials and methods

2.1. Synthesis of gelatin methacryloyl (GelMA)

GelMA was synthesized as previously described [28,30]. Briefly, a 10% (w/v) porcine gelatin (Sigma-Aldrich, St. Louis, MO, USA) was dissolved in phosphate buffered saline (PBS) and heated at 60 °C for 20 min. Drop-wise addition of 8% (v/v) methacrylic anhydride (Sigma-Aldrich, St. Louis, MO, USA) under continuous stirring at 50 °C for 3 h was followed by dilution with PBS and dialysis against deionized water at 40–50 °C for 7 days. After sterile filtration and lyophilization for 4 days, GelMA was stored at −80 °C until experimental use.

2.2. Preparation and characterization of GelMA hydrogels

Freeze-dried GelMA prepolymer was dissolved in PBS at concentrations of 10, 15, 20 or 25% (w/v). After addition of 0.5% (w/v) 1-[4-(2-Hydroxyethoxy)-phenyl]-2-hydroxy-2-methyl-1-propane-1-one (Irgacure 2959, BASF, Florham Park, NJ, USA) as photoinitiator and dissolving at 80 °C, the prepolymer solutions were photocrosslinked through UV light irradiation (Omnicure S2000, 320–500 nm filter, EXFO Photonic Solutions Inc., Quebec, Canada) to form hydrogels. For visualizing porosity, circular GelMA hydrogel samples (5 mm in diameter) were fabricated, freeze-dried, sputter-coated with gold and imaged by using a FEI/Philips XL30 FEG scanning electron microscope (SEM) at 15 KV. Mechanical testing of GelMA samples was conducted as previously published [37]. Briefly, GelMA prepolymer solution was photocrosslinked to produce the following geometries: discs for compressive testing ($n = 5$; 6 mm in diameter and 1.5 mm in height) and cuboids for tensile testing ($n = 5$; 3 mm in width, 14 mm in length, and 1.5 mm in thickness). The hydrogels were either directly analyzed or stored in PBS at 37 °C for 24 h before being examined on an Instron mechanical tester (Instron 5542, Norwood, MA, USA). The strain rate was set to 0.3 mm/min for compressive testing and 1 mm/min for tensile testing. The compressive strength and the ultimate tensile strength of the samples were determined at the point of failure (rupture under tensile and compressive loading) of the hydrogels. The compressive modulus was calculated based on the slope in the linear portion of the stress/strain curves up to a 0.2 strain.

In order to analyze the swelling characteristics, GelMA hydrogel samples ($n = 5$) were allowed to swell in PBS at 37 °C for 1, 2 or 3 days. At the end of the experiment, excess liquid was gently removed, and the wet weight was measured. After lyophilization, the dry weight of the samples was measured, and the swelling ratio was calculated as (wet weight-dry weight)/dry weight.

The crosslinking degree of GelMA in dependency on the crosslinking time was assessed by proton nuclear magnetic resonance (^{1}H NMR) analysis. GelMA hydrogels were prepared at 25% (w/v) polymer concentration and different ultraviolet (UV) exposure time (0.5, 1, 2, 3 min). Uncrosslinked GelMA prepolymer was dissolved in D_2O at a concentration of 10 mg/ml. For crosslinked GelMA hydrogels, deuterated dimethyl sulfoxide was used to partially dissolve the hydrogels prior to ^{1}H NMR analysis. In order to quantify the degree of crosslinking, all spectra were normalized with respect to the phenylalanine signal ($\delta = 6.9–7.3$ ppm). According to previous studies, the signals related to methacrylation appear at three different peaks including two protons of methacrylate double bonds located at $\delta = 5.30$ and 5.7 ppm, and the methyl function of the methacrylate group at $\delta = 1.91$ ppm [38,39]. The degree of crosslinking was calculated as below:

$$\text{Degree of Crosslinking (DC)\%} = \left(1 - \frac{\text{Area(methacrylate groups)}}{\text{Area(phenylalanine signal)}}\right) \times 100,$$

which represents the ratio of remaining C=C in the methacrylated groups after the crosslinking process.

2.3. Wound closure test

The adhesion strengths of GelMA and the clinically available surgical sealants Evicel® (Ethicon, Somerville, NJ, USA), Progel™ (NeoMend, Ervine, CA, USA) and Coseal™ (Baxter, Deerfield, IL, USA) were examined by using the standard test method for wound closure strength of tissue adhesives and sealants, ASTM F2458-05, with some modification. In brief, fresh porcine skin from a local slaughterhouse was prepared by removing the adipose tissue layer and cutting the sample into rectangular sections (5 mm × 15 mm). While unused, porcine skin was kept moist in gauze soaked in PBS. Before use, porcine skin was blotted dry to remove excess liquid, and each end of the skin strip was fixed onto two poly(methyl methacrylate) slides (30 mm × 60 mm) with Krazy glue (Westerville, OH, USA), leaving a 6 mm section of skin between the slides. The porcine skin strip was then cut apart using a razor blade (Fig. S3), and petroleum jelly was applied with a syringe to the ends of the desired adhesive application area in order to confine the prepolymer before crosslinking. Afterwards, 40 μl of the desired adhesive to be tested was applied on the tissue, and in the case of GelMA sealant, was irradiated with UV light.

The control glues were applied according to the manufacturers' instructions: For Evicel® sealant, separate vials of thrombin and fibrinogen were thawed, placed into the applicator, and allowed to mix and polymerize as they were sprayed onto tissue. For Coseal™ sealant, two components of PEG were allowed to mix within the applicator as they were applied onto tissue and polymerized on contact. For Progel™ sealant, human serum albumin and a PEG crosslinker were kept in two separate components, and were mixed when sprayed onto tissue and cured upon contact. After 1 h of incubation in PBS, the two plastic slides were placed into an Instron mechanical tester, with special attention paid to the placement of the two sides of the samples in order to minimize the effect of any additional stress due to misalignment. The adhesive strength of a sealant sample was determined at the point of tearing using a strain rate of 1 mm/min. Each tested adhesive group contained four to seven samples.

2.4. Lap shear test

The shear strength of GelMA sealant, Evicel®, Progel™ and Coseal™ was examined according to the standard test method for strength properties of tissue adhesives under lap-shear by tension loading, ASTM F2255-05. Gelatin coating solution was prepared by dissolving porcine gelatin 20% (w/v) in PBS at 80 °C. The top region (10 mm × 15 mm) of two glass slides (10 mm × 50 mm in total) was

coated with gelatin, which was allowed to dry at room temperature [40]. Afterwards, 20 μl of the desired adhesive was applied on a 10 mm × 10 mm area on top of the gelatin coating of one glass slide (Fig. S4), after which another gelatin-coated glass slide was placed over the adhesive, and in the case of GelMA sealant, was followed by irradiation with UV light. The two glass slides were placed into an Instron mechanical tester for shear testing by tensile loading with a strain rate of 1 mm/min. The shear strength of the sealant sample was determined at the point of detaching. Each tested adhesive group contained five samples.

2.5. In vitro burst pressure test

The burst pressure of GelMA sealant, Progel™, Evicel® and Coseal™ was tested by using a standard test method for burst strength of surgical sealants, ASTM F2392-04. Collagen sheets (40 mm × 40 mm) were soaked in PBS prior to sample preparation. A circular defect (3 mm in diameter) was created in the center of a collagen sheet that was placed between two Teflon sheets (35 mm × 35 mm) (Fig. S5). 50 μl of the desired adhesive solution was injected on the defect and, in the case of GelMA, the prepolymer was irradiated with UV light. Afterwards, the collagen sheet was placed into the burst pressure testing system, consisting of a pressure detection and recording unit and a syringe pump, that applied air with continuously increasing pressure towards the samples until bursting. Each tested adhesive group contained five samples.

2.6. In vitro degradation test

The *in vitro* degradation was examined by means of a collagenase-based assay. Disc-shaped GelMA samples (d = 5 mm; h = 4 mm) with prepolymer concentrations of 10, 15, 20 and 25% (w/v) were formed by using different UV crosslinking times ranging from 0.5 to 3 min. After dry weight measurement, the samples were incubated with 2 μg/ml collagenase (in PBS) for 1, 3, 5, 7 or 10 days (n = 3 per condition and observation period). At the end of the incubation period, the dry weight of the samples was measured again, and their degradation was calculated based on the weight loss.

2.7. Cytotoxicity of uncrosslinked GelMA prepolymer

In order to test the cytotoxicity of the GelMA prepolymer, various concentrations of GelMA (10, 15, 20 and 25% (w/v)) were prepared in Dulbecco's Modified Eagle's medium (DMEM) cell culture media. The solutions were transferred into 24 well plates, and 3000 3T3 cells per μl were added (100 μl). The cell viability was assessed after 24 h using a calcein-AM/ethidium homodimer live/dead assay.

2.8. Animal experiments

All small animal experiments were conducted in male Wistar rats weighing 200–250 g, obtained from Charles River (Wilmington, MA, USA), housed in a local animal care facility (PRB, Cambridge, MA, USA) and fed *ad libitum*. Anesthesia and analgesia were initiated and supported by isoflurane inhalation (2.0–2.5% (v/v)) and subcutaneous carprofen administration (5 mg/kg/d). The large animal experiments were performed on 3 pigs weighing 40–50 kg, obtained from Parsons farms (MA, USA), housed in a local animal care facility (ARF at Beth Israel Deaconess Medical Center, Boston, MA, USA) and fed *ad libitum*. Anesthesia and analgesia were initiated and supported by isoflurane inhalation (5% → 1–3% (v/v)) and intramuscular tiletamine/zolazepam administration (6.6 mg/kg). Postprocedural analgesia was maintained by fentanyl-TTS (2–4 μg/kg) and intramuscular buprenorphine (0.03 mg/kg).

All experiments strictly followed the NIH "Guide for the Care and Use of Laboratory Animals" and were approved by the local animal care committees (HMA Standing Committee on Animals and Institutional Animal Care and Use Committee at Beth Israel Deaconess Medical Center; protocol numbers 05055 and 029-2015).

2.9. Subcutaneous implantation of GelMA hydrogels in rats

Subcutaneous implantation of GelMA in rats (n = 6) was conducted as recently published [36,41]. After induction of general anesthesia, small separated subcutaneous pockets were bluntly prepared through short dorsal skin incisions (10 mm in length), and 25% (w/v) GelMA samples (n = 18) were implanted. After anatomical wound closure, the animals were allowed to recover from anesthesia. After 3, 7 or 28 days, the animals were euthanized by CO_2 inhalation, and the implants including adjacent tissue were explanted and further processed for histology.

2.10. Evaluation of the performance of GelMA sealant in a rat lung leakage model

In order to examine the suitability and effectiveness of GelMA as sealant for lung leakages *in vivo*, a rat model was developed based on previous literature [27]. After induction of inhalative anesthesia, rats were orally intubated and subsequently ventilated (frequency 80 per min; tidal volume 3 ml) maintaining isoflurane anesthesia. Through a right lateral thoracotomy in the sixth intercostal space, a standardized lung lobe incision (3 mm in length; 5 mm in depth towards the hilum) was generated with a No.11 surgical blade. All animals showed outbreak of air bubbles and small amounts of blood through the incisions. Immediately, under ventilation arrest, 50 μl GelMA prepolymer solution (n = 7), Evicel® (n = 3) or Progel™ (n = 6) was administered and cured for 2 min for Progel™, or 0.5 min in case of GelMA under UV light (Fig. 4a and b). As additional control, leaking lungs (n = 6) were sutured with a "Z" stitch using 6-0 polypropylene sutures (Ethicon, Somerville, NJ, USA). After having re-established ventilation, leakage from the sealed injury was tested by application of warm saline solution, whereas no leakage was detected after single use of the sealants in any of the animals. The thorax was anatomically closed, followed by de-airing of the pleural space by means of a custom-made thorax drainage system. In case of chronic experiments, animals were allowed to recover from anesthesia under sustained ventilation.

Directly after defect sealing (n = 18), at day 7 (n = 6) and day 28 (n = 3), the animals were euthanized. Histology and immunohistology were performed from explants at day 7 (n = 3) and day 28 (n = 3), and burst pressure measurements were conducted at day 0 (n = 18) and day 7 (n = 3). For burst pressure testing, the trachea was occlusively intubated and connected to a split tubing system linking a pressure detection and recording unit and a syringe pump with the lungs of the rat (Fig. 4c). Under continuous air injection, the lungs were inflated, and the increasing pressure was recorded up to the point of material burst or detachment or tissue burst. The time point and type of sealant failure was additionally visualized by conducting the experiment in a water bath, resulting in air bubbles rising from the leakage site. Burst pressure measurements in non-injured lungs (n = 3) served as additional controls.

2.11. Evaluation of the performance of GelMA sealant in a porcine lung leakage model

Intending translational analysis, GelMA was tested in a

previously published chronic porcine lung leakage model [25]. After induction of general anesthesia, pigs were orally intubated and subsequently ventilated (frequency 20 per min; tidal volume 10 ml/kg) maintaining isoflurane anesthesia. Through a right lateral thoracotomy, a standardized visceral pleural defect (15 mm in length; 15 mm in width; 1 mm in depth) was generated with a scalpel (Fig. 5a). All animals showed outbreak of air bubbles (d > 2 mm) and small amounts of blood through the incisions during a submersion test with intrapleural warm saline solution (Fig. 5b). Immediately, under ventilation arrest, 500 μl GelMA (n = 3) was administered and cured for 1 min under UV light (Fig. 5c). After having re-established ventilation, leakage from the sealed injury was tested again by application of warm saline solution, whereas no leakage was detected after single use of the sealants in any of the animals. The thorax was anatomically closed, followed by de-airing of the pleural space by means of a thorax drainage system. Afterwards, animals were allowed to recover from anesthesia under sustained ventilation. The surgical procedure is presented in Video S1.

Supplementary video related to this article can be found at http://dx.doi.org/10.1016/j.biomaterials.2017.06.004.

Pleural ultrasound imaging was performed on postoperative days 7 and 14 to exclude a pneumothorax, using an Acuson Sequoia C512 sonography system (Siemens Healthcare, Erlangen, Germany). Fourteen days after surgery, following humane euthanasia of the animals, the sealed defect area was excised and further processed for histology.

2.12. Histology and immunohistology

Histology and immunohistology were conducted on paraformaldehyde-fixed 4–6 μm paraffin and cryo-sections of the explants as previously reported [42]. Hematoxylin/eosin (H & E) staining was performed to obtain microscopic overview. Masson trichrome staining allowed for depicting of connective tissue. For immunohistology, the primary antibodies anti-CD3, anti-CD68 (both from Abcam, Cambridge, MA, USA) and anti-Mac-2 (Cedarlane, Burlington, ON, Canada), and Alexa Fluor®-conjugated secondary antibodies (Life Technologies, Carlsbad, CA, USA) were used. Immuno-labelled sections were covered with DAPI-containing Vectashield mounting medium (Vector Labs, Peterborough, United Kingdom) and visualized on a LSM 880 confocal microscope (Zeiss, Jena, Germany).

2.13. Statistics

Continuous variables displayed as mean values ± standard deviations. Group comparisons were conducted by one-way-ANOVA with Bonferroni post-hoc tests. P-values <0.05 were assumed to indicate significance. Data analysis was conducted with GraphPad Prism (GraphPad Software, La Jolla, CA, USA).

3. Results

3.1. Physical characteristics of GelMA sealant

Prior to the examination of the suitability of GelMA hydrogels to act as sealants, the physical properties of engineered hydrogels in dependency on different GelMA concentrations (10, 15, 20 and 25% (w/v)) were tested. Freshly photocrosslinked hydrogels and hydrogels soaked in PBS for 24 h underwent compressive mechanical testing. Under both conditions, higher GelMA concentrations resulted in increased values for the compressive modulus (from 36 ± 16 kPa for 10% GelMA to 156 ± 48 kPa for 25% GelMA) and compressive strength (Figs. S1a and b). The highest compressive strength (1018 ± 167 kPa) was obtained for a 25% (w/v) GelMA hydrogel (Fig. S1b). After 24 h of incubation in PBS, a 10–15% drop in compressive strength was observed for all GelMA formulations, as shown in Fig. S1b. Tensile testing also revealed the highest elastic modulus (180 ± 34 kPa) and increased ultimate tensile strength (53 ± 17 kPa) for a 25% (w/v) GelMA when compared to other GelMA formulations (Figs. S1c and d). In addition, the elasticity of GelMA hydrogels varied between 30% and 40% as the GelMA concentration was changed from 10% (w/v) to 25% (w/v) in uniaxial tensile tests (Fig. S1c).

The swelling ratios of GelMA hydrogels at different concentrations were calculated by dividing the measured weights of the hydrogel samples after 1–3 days of incubation at 37 °C in PBS by their corresponding dry weights. As shown in Fig. S1e, the swelling ratios of the hydrogels decreased with increasing GelMA concentrations. However, the swelling ratio values changed only slightly over time, indicating that equilibrium states were achieved after 24 h. SEM images of the GelMA hydrogels revealed the resulting hydrogels having highly porous structures (Fig. S1f).

Based on ^{1}H NMR analysis, the degree of crosslinking was calculated from the disappearance of the C=C bonds correlated to the methacrylated groups at δ = 5.30 and 5.7 ppm. The degree of crosslinking was above 78% after 0.5 min UV exposure time. Furthermore, after 1 min reaction time, 84% of the originally methacrylated groups were consumed (Fig. S2). Interestingly, the degrees of crosslinking were 92% and >95% after 2 min and 3 min, respectively, indicating that the reaction rate decreased over time. Overall, the hydrogel crosslinking was approximately completed (>95%) after 3 min UV exposure time. Therefore, we used 3 min as the optimal reaction time to form fully crosslinked hydrogels for the following experiments.

3.2. In vitro adhesion strength, shear strength and burst resistance of GelMA sealant

Properties that are important for effective sealants, including adhesion strength, shear strength, and burst pressure, were examined *in vitro* according to ASTM standard tests. In these tests, the sealing capability and adhesion strength of GelMA sealants, produced by using different GelMA concentrations and photocrosslinking times, were compared to the clinically established sealants such as Evicel®, Coseal™ and Progel™.

The adhesion strength of the engineered sealants was measured by using a modified wound closure test based on ASTM F2458-05 (Fig. S3). Higher concentrations of GelMA led to higher adhesive strengths. Specifically, the 25% GelMA hydrogels, that was crosslinked by using 3 min light exposure time, attained an adhesive strength of 49 ± 9 kPa, which was higher than those of Evicel® (19 ± 17 kPa) and Coseal™ (26 ± 5 kPa) and lower than that of Progel™ (78.7 ± 14 kPa) (Fig. 1a). In addition, it was found that the adhesive strength was also slightly affected by the light exposure time (Fig. 1b): a 23% enhancement in adhesion strength (from 40 ± 5 kPa to 49 ± 9 kPa) was observed when the exposure time increased from 0.5 to 3 min for a 25% GelMA hydrogel, but this was not statistically significant.

The shear strength of the engineered sealants was also characterized by using a modified lap shear test based on ASTM F2255-05 (Fig. S4). Similar to the wound closure test, the highest shear strength was obtained for the 25% (w/v) GelMA (262 ± 55 kPa) photopolymerized by using 3 min light exposure time, which was significantly higher than for Evicel® (207 ± 67 kPa), Coseal™ (70 ± 21 kPa) and Progel™ (226 ± 33 kPa) (Fig. 1c). In addition, increasing the UV exposure time from 0.5 to 3 min enhanced the shear strength of a 25% GelMA sealant from 175 ± 23 kPa to 262 ± 55 kPa as shown in Fig. 1d.

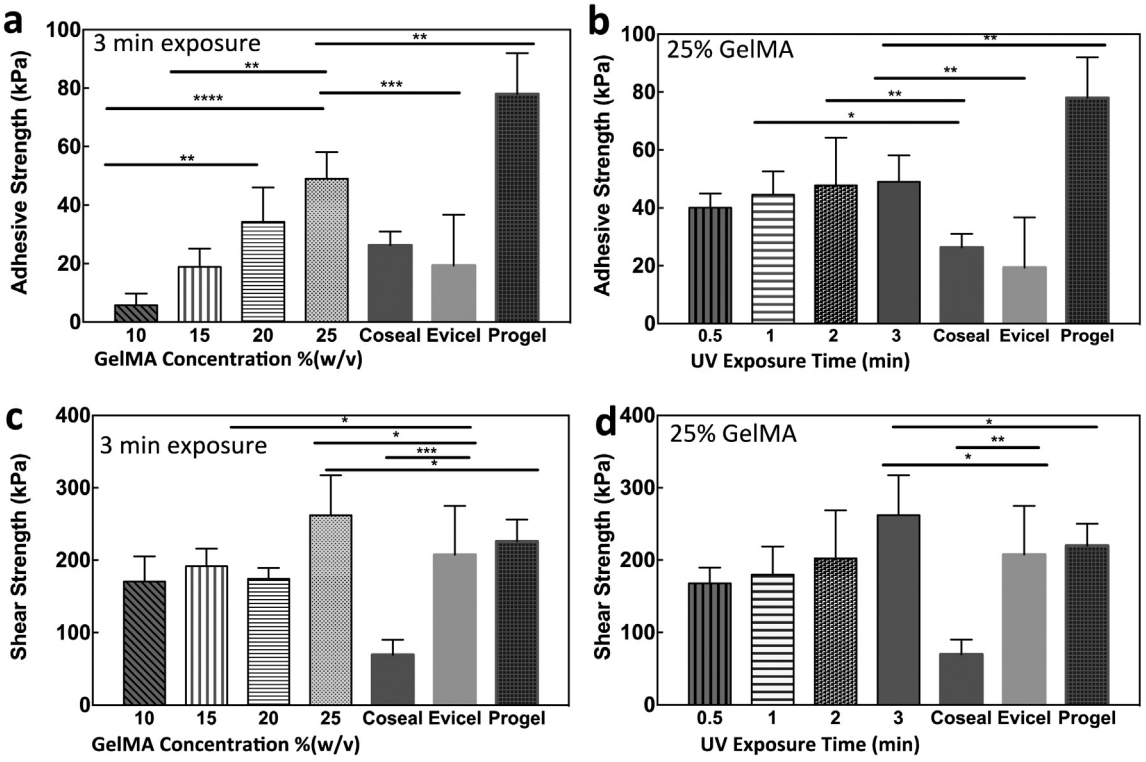

Fig. 1. *In vitro* sealing properties of GelMA sealant. (**a,b**) Standard wound closure test using porcine skin as a biological substrate to test the *in vitro* adhesion strength of GelMA and different commercially available sealants. (**c,d**) Standard lap shear test to determine the shear strength of GelMA sealant in comparison to different commercially available sealants. The effect of GelMA prepolymer concentrations on the adhesion strength of hydrogels formed at 3 min UV exposure time is shown in **a,c**; the effect of the UV exposure time on the adhesion strength of a 25% GelMA sealant is shown in **b,d**. (*p < 0.05, **p < 0.01, ***p < 0.001, ****p < 0.0001).

In order to test the burst pressure of the engineered sealant, continuously increasing air pressure was exerted on sealants covering a standardized defect in a collagen sheet based on ASTM F2392-04 (Fig. S5). The burst pressure of GelMA sealant significantly enhanced from 3.0 ± 0.6 kPa to 14.9 ± 5.7 kPa as the GelMA concentration was increased from 10% (w/v) GelMA to 25% (w/v) GelMA at 3 min light exposure time (Fig. 2a). In addition, a 25% (w/v) GelMA sealant outperformed all three commercially available adhesives, reaching a burst pressure of 14.9 ± 5.7 kPa compared to 1.5 ± 0.7 kPa for Evicel®, 1.6 ± 0.2 kPa for Coseal™, and 4.4 ± 0.4 kPa for Progel™ (Fig. 2a). It should be noted that even at the lowest tested concentration (10%), the burst pressure of GelMA was two-fold higher than those of Evicel® and Coseal™. Moreover, the burst pressure value for a 25% GelMA sealant was enhanced approximately 5-fold by increasing the UV exposure time from 0.5 to 3 min (Fig. 2b).

Taken together, the mechanical testing and ASTM standard tests for adhesives showed excellent mechanical and adhesive properties for GelMA sealants produced by using 25% GelMA prepolymer concentration. The wound closure strength, the shear resistance and especially the burst pressure were significantly higher for a 25% (w/v) GelMA sealant as compared to clinically available PEG-based and fibrin-based control glues. Therefore, this formulation was used for the *in vivo* examination of its biocompatibility using a rat subcutaneous implantation model and its biofunctionality using a lung incision model in both small and large animals.

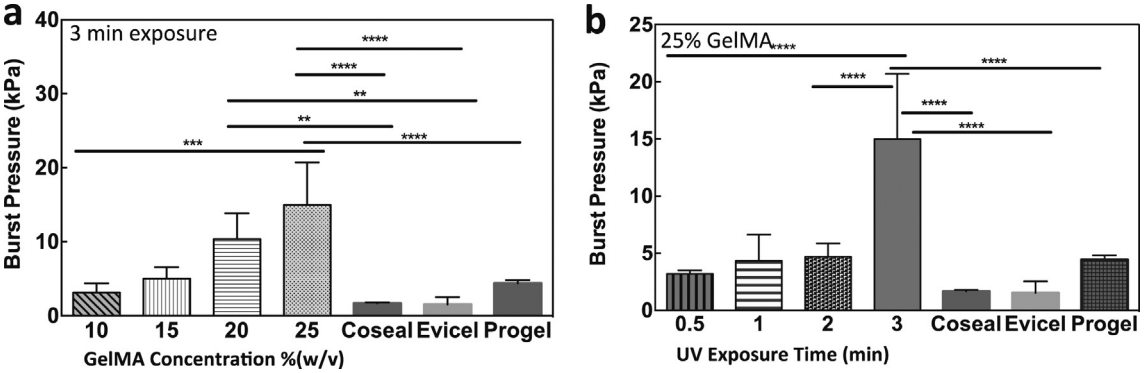

Fig. 2. *In vitro* burst pressure of GelMA sealant. Burst pressure values for commercially available sealants and GelMA sealants produced by **(a,b)** varying GelMA concentrations at 3 min UV exposure time and **(c,d)** changing UV exposure time for a 25% GelMA sealant. (**p < 0.01; ***p < 0.001; ****p < 0.0001).

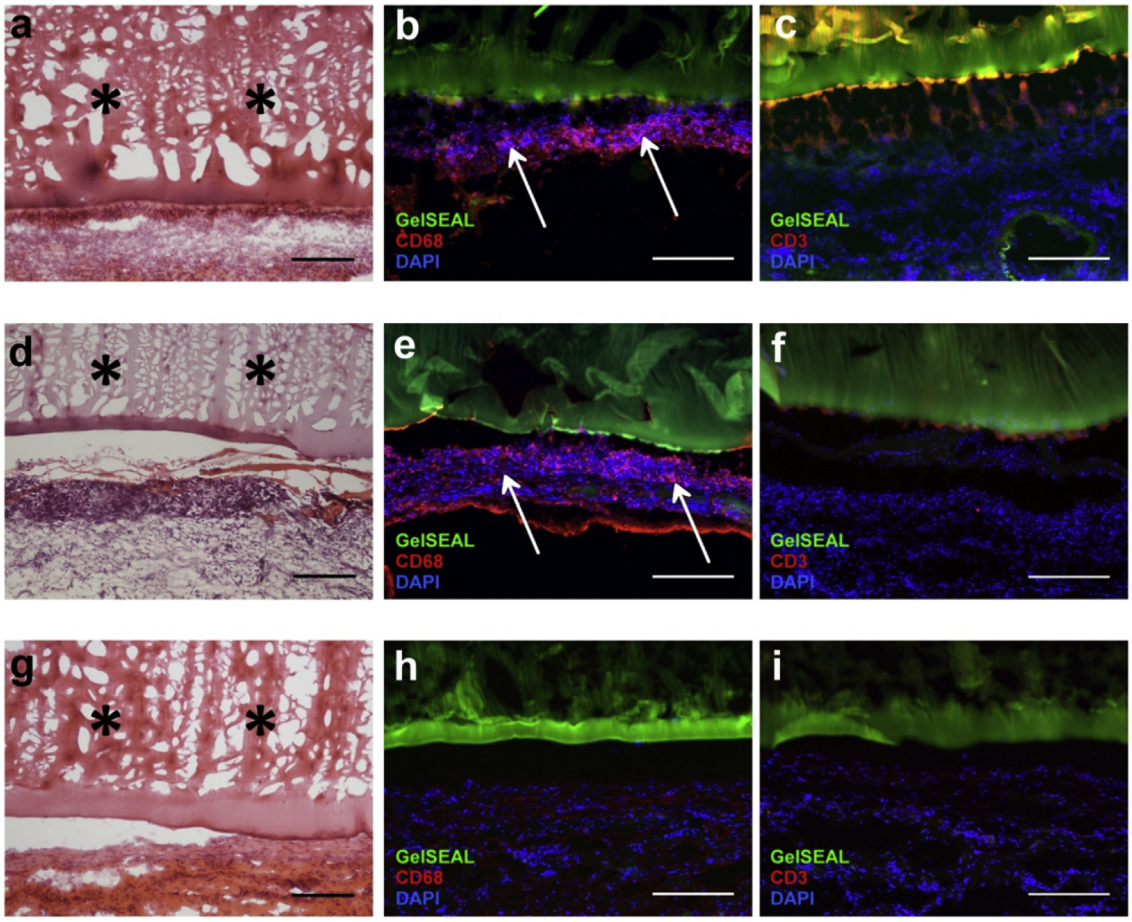

Fig. 3. *In vivo* biocompatibility of GelMA sealant. Immunohistology analyses **(a–c)** 3, **(d–f)** 7, and **(g–i)** 28 days after subcutaneous implantation in rats showed initial implant-surrounding macrophage (CD68) invasion (arrows in **b,e**), which was no longer present at day 28 **(h)**. At no point were there signs of lymphocyte (CD3) infiltration **(c,f,i)**. (**a,d,g,** H & E staining; asterisks, GelMA sealant; scale bars, 200 μm).

3.3. In vitro degradation of GelMA sealant

The degradation of the GelMA hydrogels was examined using a collagenase-based *in vitro* assay. Low prepolymer concentrations ($p < 0.0001$) and short UV crosslinking times ($p < 0.0001$) resulted in significantly accelerated degradation as compared to higher concentrations and longer crosslinking times (Fig. S6) (Table S1).

3.4. Cytotoxicity of uncrosslinked GelMA prepolymer

The cytotoxicity of uncrosslinked GelMA prepolymer was examined by using 3T3 cells and a live/dead assay for different prepolymer concentrations. As shown in Fig. S7, after one day of incubating 3T3 cells with different concentrations of GelMA prepolymer solutions, high cell viability was observed for all tested conditions, confirming that uncrosslinked GelMA prepolymer did not induce cytotoxicity.

3.5. Biocompatibility of GelMA sealant in rats

The *in vivo* biocompatibility of GelMA sealant was examined 3, 7 and 28 days after subcutaneous implantation of the hydrogels in rats. Histological staining revealed no relevant monocyte infiltration around or into the sealant (Fig. 3a,d,g). At days 3 and 7, macrophages were observed around the implants (Fig. 3b,e); however, at day 28, they were no longer present (Fig. 3h). At all time points, no lymphocyte infiltration was detected (Fig. 3c,f,i).

3.6. GelMA sealant for lung leakages in a rat model

A rat model of standardized lung leakage was established to test the suitability and effectiveness of GelMA sealant for *in vivo* sealing of pulmonary lesions in the absence of any additional conventional surgical methods, for example, suturing or stapling (Fig. 4a and b). The initial sealing strength of GelMA as well as the burst pressure of the sealed lung tissue during autologous defect repair at the post-operative day 7 were examined. All rats survived the surgery and the desired follow-up period up to day 28. No clinical signs of post-operative pneumothorax were observed, and at the end of the follow-up period, no lung leakage was found. In order to quantify the sealing strength, burst pressure measurements were conducted on the GelMA-sealed lungs on day 0 and day 7, and on healthy lungs as controls (Fig. 4c–e). Evicel®, Progel™ and polypropylene sutures only were used as controls in this experiment. In the case of GelMA, the typical mode of failure was not bursting of the material, but rather detachment from the lung surface at a burst pressure value of 5.7 ± 1.5 kPa, or bursting of native lung tissue outside of the defect area (Fig. S8a). On the contrary, Evicel® and Progel™ failed by direct material bursting at 2.7 ± 0.7 kPa and 2.2 ± 0.7 kPa, respectively, which was due to the low mechanical properties of the adhesives (Fig. S8b). In case of sutures, the lung tissue burst around the stitch channels at 3.1 ± 0.7 kPa. The burst pressure of GelMA sealant immediately after curing on the lung tissue was significantly higher in comparison to Evicel® ($p < 0.01$), Progel™ ($p < 0.001$) and sutures

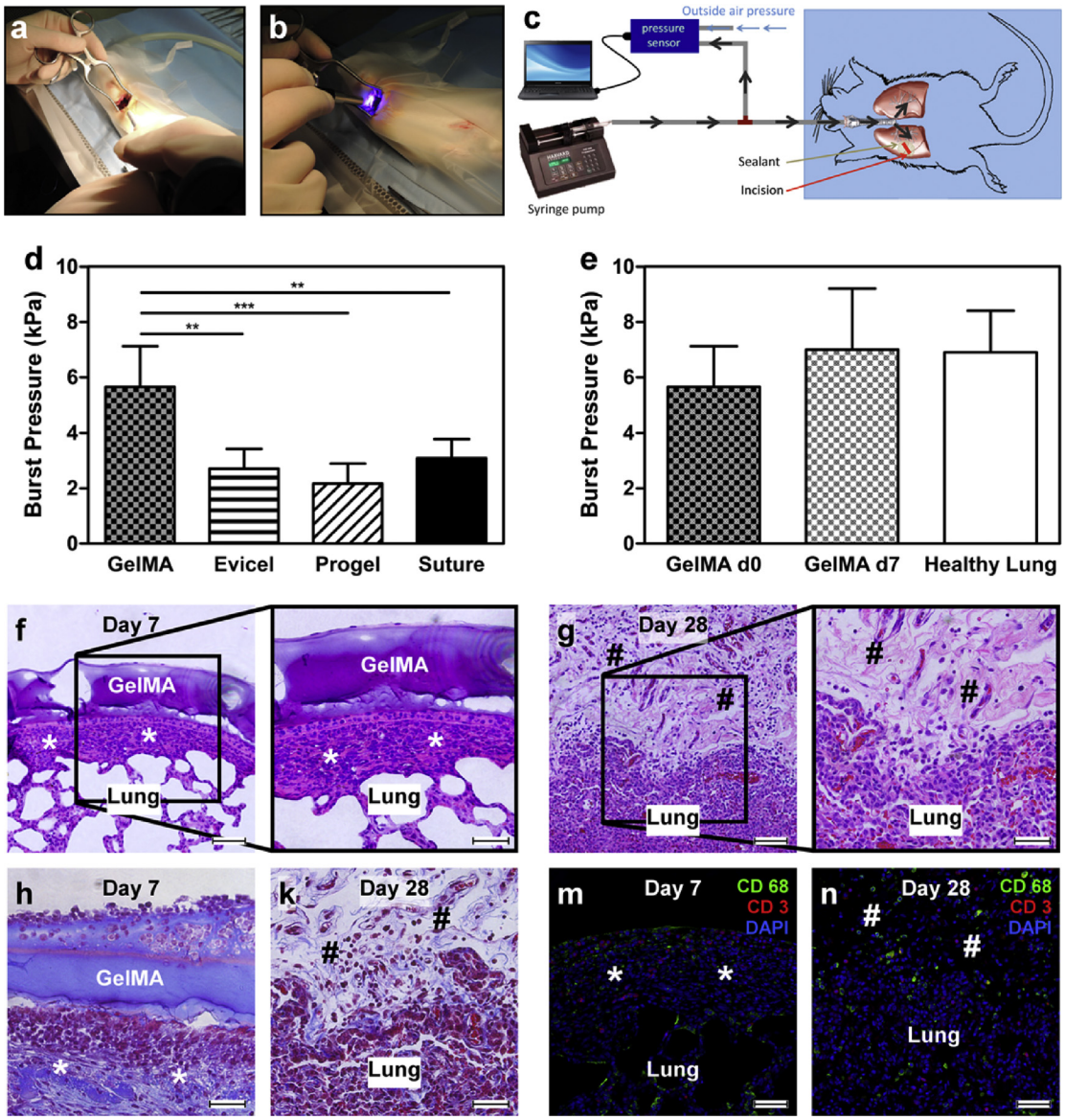

Fig. 4. ***In vivo*** **sealing capacity of GelMA sealant using a rat lung incision model.** (**a**,**b**) GelMA sealant is applied on a lung leakage via a small lateral thoracotomy and UV-crosslinked until the incision was sealed. (**c**) Schematic of the setup used to measure the lung burst pressure after sealing: A syringe pump and a pressure sensor are connected to the trachea allowing for pressure monitoring during lung inflation in a closed system. (**d**) Burst pressure of GelMA-sealed, Evicel®-sealed, Progel™-sealed and sutured lungs immediately after material application demonstrating that the burst pressures of GelMA sealant-treated lungs were significantly higher than those in all other groups. (**e**) Burst pressure of GelMA-sealed lungs on day 0 and day 7 post surgery compared to healthy lung: 7 days after surgery, the burst pressure of GelMA-sealed lungs was further increased as compared to day 0 and reached the level of healthy lung tissue. (**f**,**g**) H & E and (**h**,**k**) masson trichrome stainings of GelMA-sealed lung tissue sections at days 7 and 28. Histologically, defect repair tissue was observed under the GelMA cover 7 days after lung leakage sealing (asterisks in **f**), including stable collagenous tissue layers (asterisks in **h**). After 28 days *in vivo*, host cells had invaded the GelMA seal and matrix remodeling had occurred (hashs in **g**,**k**). Immunohistology of GelMA-sealed lung tissue sections at **(m)** day 7 and **(n)** day 28 revealed only sparse presence of CD3- and CD68-positive cells around the GelMA implants (asterisks in **m**, defect repair tissue; hashs in **n**, remodeled hydrogel cover). (scale bars, 100 μm and 50 μm in the high magnification pictures, respectively; **$p < 0.01$; ***$p < 0.001$).

only ($p < 0.01$) (Fig. 4d). Due to the extensive air leakages from the Evicel®- and Progel™-sealed lung tissue, leading to lethal pneumothorax shortly after extubation, the chronic survival tests were continued by using 25% GelMA sealant only. Seven days after surgery, the burst pressure of GelMA-sealed lung tissue was even further elevated as compared to day 0 and reached values that were equal to the burst pressure of native healthy rat lung tissue (7.0 ± 2.2 kPa versus 6.9 ± 1.5 kPa) (Fig. 4e). In some burst pressure experiments on GelMA-sealed lungs, it was not the sealant that had failed, but instead the native lung tissues had burst in other areas. Therefore, the reported burst pressure value is the actual rat lung burst pressure. This observation highlights the need for using a large animal model for accurate testing of the performance and sealing capability of the engineered sealants.

Histology assessment of the sealing area revealed stable collagenous defect repair tissue under the GelMA cover at day 7 after sealing, while at day 28, cellular invasion into the hydrogels and consecutive matrix remodeling were observed (Fig. 4f–k). Immunohistology demonstrated that only a minor number of the invading cells had an inflammatory phenotype (Fig. 4m and n).

3.7. GelMA sealant for lung leakages in a translational pig model

A translational porcine lung lesion model was used to further

demonstrate the suitability of a 25% GelMA hydrogel as a lung sealant without the use of any additional conventional surgical methods such as suturing or stapling (Fig. 5a–c, Video S1). Three pigs were tested and all animals survived the surgery and the desired follow-up period of 14 days. No clinical or sonographic signs of pneumothorax were observed during the follow-up (Fig. 5d–e). After 14 days, the defect sites were covered by connective repair tissue, while GelMA sealant had disappeared.

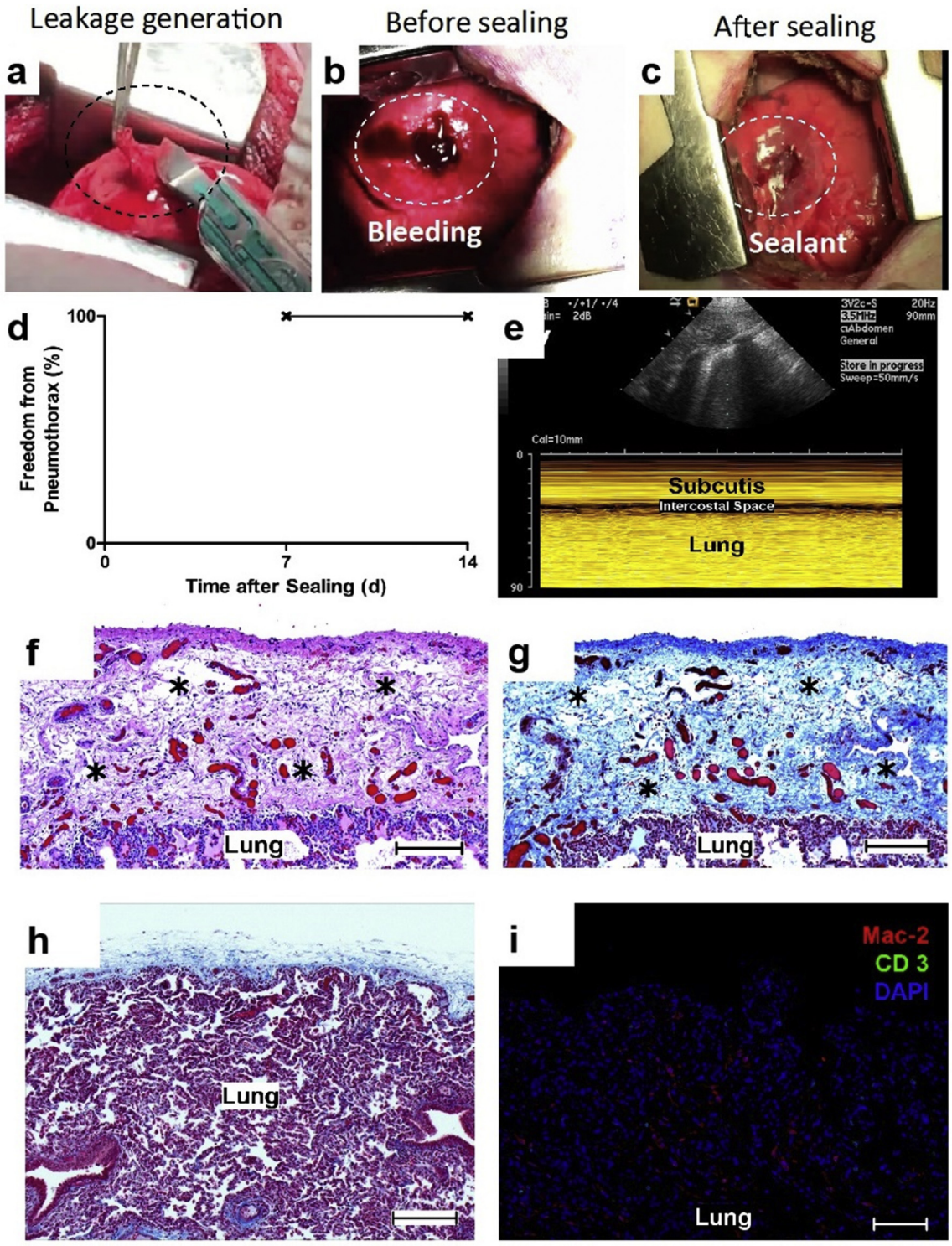

Fig. 5. ***In vivo*** **sealing capacity of GelMA sealant using a porcine lung incision model.** (**a-c**) A right lung lobe is exposed via a small lateral thoracotomy, a standardized defect is created (broken lines in **a** and **b**) and sealed by photocrosslinking of GelMA sealant (broken line in **c**). (**d,e**) Ultrasound studies on the sealed lung tissue at postoperative days 7 and 14: Freedom from pneumothorax was confirmed by sonography, as shown in a representative ultrasound image at day 14. (**f-h**) Representative histological sections of the GelMA-sealed site after 14 days revealed sufficient wound healing (asterisks in **f**) including a stable collagenous (blue) defect cover (asterisks in **g**), in comparison with non-injured parenchymatous lung tissue (**h**). For high magnification pictures, see Fig. S9. (**i**) By immunohistological staining of the GelMA-sealed tissue, no lymphocyte infiltration (CD3) was observed, and only mild macrophage accumulation (Mac-2) occurred. (**f**, H & E staining; **g,h**, masson trichrome staining; scale bars in **f,g,h**, 200 μm; scale bar in **i**, 100 μm). (For interpretation of the references to colour in this figure legend, the reader is referred to the web version of this article.)

Histological evaluation of the injured area revealed strong collagenous defect repair tissue (Fig. 5f–g) (Fig. S9), whereas the surrounding area exhibited healthy lung parenchyma (Fig. 5h). Immunohistology revealed no signs of lymphocyte infiltration and only mild macrophage accumulation in the sealed defect area (Fig. 5i).

4. Discussion

The use of a gelatin-based adhesive to seal lung defects has been recently suggested [25]. Photopolymerization of tyrosine-enriched gelatin in the presence of ruthenium and SPS has resulted in hydrogels with promising tensile and adhesive characteristics. However, the *in vivo* toxicity of ruthenium and SPS caused a mild inflammatory response after sealing of sheep lung defects. Furthermore, the developed ruthenium and SPS sealant was used only with additional sutures and no control group without the adhesive was tested. Although adequate sealing of sheep lung tissues was claimed when using the engineered gelatin-based sealant, the reported results were described only qualitatively. In summary, this previous gelatin-based adhesive sealed lung leakages only in the presence of additional sutures, and caused mild local inflammation. In contrast, the GelMA sealant in our study was examined in a rat lung leakage model without additional use of sutures or staples. A single application of GelMA sealant with only 50 μl of prepolymer outperformed fibrin glue, Progel™, and polypropylene sutures with a two-fold increase in burst pressure directly after curing of the sealants. The burst pressure values of GelMA-sealed lung tissues reached a level that was similar to that of native rat lung tissue, and at day 7 after surgery, the burst pressure of GelMA-sealed lungs was further elevated. Therefore, most of the lungs did not burst at the defect site (in contrast to fibrin glue), but in initially unimpaired tissue regions. Since by day 7, new tissue had grown on the sealed defect site, the supra-physiological burst pressure values at day 7 may not be attributed to the GelMA sealant alone. However, directly after sealing at day 0, the burst pressure levels of GelMA-sealed lungs were already close to those of healthy lungs, and the initial sealing strength was high enough to bridge the time period until defect repair by ingrowing autologous tissue.

In situ photopolymerization of the GelMA prepolymers facilitates easy delivery even to technically demanding locations, such as during minimally invasive surgery, and allows for curing of the sealant exactly according to the required geometry of the tissue to be sealed, which is an advantage over pre-fabricated materials such as hemostyptic collagen or fibrinogen/thrombin scaffolds [43,44]. Besides physical interconnection of the curing sealant with the tissue surface, gelatin offers additional interaction with tissues in defect areas. Since gelatin contains multiple domains that bind to cell-surface receptors and extracellular matrix proteins, initial connection of the sealant to the tissue as well as subsequent cell attachment to and cell growth on the sealant is promoted [45]. Gelatin has these properties in common with collagen, which it is derived from. However, xenogeneic collagen exhibits increased antigenic response as compared to xenogeneic gelatin due to its helical structure and the higher content of tyrosine, tryptophan, and phenylalanine, resulting in enhanced formation of aromatic radicals [46,47].

It has been reported that native lung tissue has an elasticity of around 40% [48,49]. As we plan to use the engineered hydrogel as a lung sealant, the 25% GelMA formulation with elasticity similar to lung tissue may be suitable for future experiments. Due to the high ultimate strength of the 25% (w/v) GelMA hydrogel, it is expected that the engineered formulation could structurally withstand the forces exerted on human lung tissue and adjacent adhesives since, even in patients under invasive ventilation, the positive pressure in the lungs rarely reaches more than 5 kPa [50]. These values are already substantially higher than the maximum pressures exerted on the lung tissue during physiological breathing, reaching values within 0.13–0.26 kPa of atmospheric pressure [51]. The optimized mechanical properties of the engineered GelMA sealant can offer certain flexibility and stiffness, which will not limit the lung tissue movement and allow normal function while minimizing tissue damage.

The significantly reduced swelling ratio in 25% GelMA sealant, as compared to other formulations, indicates improved stability of the hydrogels against swelling and may thereby avoid the risk of additional stress on the surrounding tissue by material expansion after application.

Human fibrin-based glues are probably the most widely used surgical adhesives, since they provide adequate hemostasis in many surgical scenarios and have low immunogenicity. Unfortunately, their mechanical properties are low and their production is expensive. Conversely, GelMA sealant has proven to have beneficial mechanical and adhesive properties and also a low manufacturing cost. Furthermore, the human origin of fibrin potentially allows for viral diseases transmission, such as hepatitis C or human immunodeficiency virus, although no transmission has yet been proven [11]. GelMA sealant is produced from porcine or bovine gelatin that can be harvested under sterile conditions from animals in pathogen-free barrier facilities, so that the risk of transmission or infection may be even lower than that of human fibrin-based products.

Several PEG-derived sealants have been tested experimentally as well as clinically [13–18]. FocalSeal® is a light-activated sealant that has been reported to support the closure of pulmonary air leaks after previous suturing or stapling in large animals and humans [17,18]. However, its usage without sutures or staples is not recommended. The application of FocalSeal® was approved by the Food and Drug Administration (FDA) in 2000, but due to high manufacturing costs and the need of a three step procedure for its application (the use of a primer prior to the sealant application, followed by light exposure), impeding the adoption of the sealant, the product was withdrawn from the market in 2003, even though it could be successfully used to seal lung tissue defects. Progel™, a hydrogel-based lung sealant composed of human serum albumin and a PEG derivative, has been approved by the FDA for the intraoperative application during pulmonary resection. In a rat model, it has been reported that Progel™ increases the initial lung burst pressure after sealing of a defect, when compared to fibrin glue (10.3 ± 2.5 versus 4.1 ± 2.0 kPa) [27]. In our rat study, Progel™ did not perform significantly better in comparison to the fibrin glue Evicel®. Furthermore, it was not possible to even reach the true burst pressure level of GelMA sealant, as the native rat lung tissue burst at non-defect sites before reaching this value. A multicenter trial in pulmonary resection patients showed that Progel™ application with suturing/stapling was superior to suturing/stapling only [52]. The length of hospital stay was reduced by one day, and after 30 days, 35% of the Progel™-treated lungs were leak-free (versus 14% in the control group). Although this difference was statistically significant, the 65% remaining or re-occurring leaks leave much room to improve the air leakage sealing technique with Progel™. In our study, we have shown that the burst pressure and lap shear strength of GelMA sealant were higher than those of Progel™. In addition, GelMA sealant proved to be an effective lung sealant in small and large animal models even in the absence of additional suturing/stapling. Moreover, GelMA sealant showed rat lung burst pressure values that were superior to those for polypropylene sutures only. Another disadvantage of Progel™ may be caused by the manufacturing costs for extraction and purification of human serum albumin or production of the recombinant protein,

respectively, whereas the use of Progel Platinum™ with recombinant albumin is not yet approved in the U.S. In summary, due to the above-mentioned limitations of Progel™ and the other clinically available products, it is expected that the engineered GelMA sealant in our study could be used as a biocompatible, easily applicable, and affordable surgical sealant for the sealing of soft and elastic tissues without the need for additional suturing/stapling.

The *in vitro* adhesive and cohesive properties of GelMA sealant have been examined primarily by using standard wound closure, lap shear and burst pressure. As reported in previous studies on surgical sealants, these tests were performed with standard tissues or tissue substitutes, respectively, in order to get reliable data on the general sealing potential of the gelatin-based adhesives [53–55]. Aiming to determine the sealing potential of GelMA hydrogels on the target tissue lung, additional *in vivo* experiments were conducted in two different animal models with lung lesions.

In order to translate GelMA application towards human use, the present study particularly evaluated the *in vivo* performance of the engineered hydrogel sealant in a porcine lung leakage model. The experiments proved that GelMA is suitable for the sealing of significant pulmonary defects in large animals in the absence of additional suturing/stapling and facilitated fast wound healing.

The findings on the high biocompatibility of GelMA sealant in chronic small as well as large animal models confirmed multiple reports on the beneficial biocompatibility of gelatin, which was obviously not impaired by methacrylation and UV light-mediated crosslinking [56]. GelMA hydrogels did not exert cytotoxicity, as has been shown previously [28,35]. Additionally, our data demonstrated that uncrosslinked GelMA prepolymers at different concentrations did not induce detectable cytotoxicity. In the present study, subcutaneous implantation experiments revealed moderate macrophage accumulation around the GelMA implants on days 3 and 7 that disappeared by day 28. Concordantly, there was mild macrophage infiltration on days 7 and 28 after lung leakage sealing in rats and on day 14 after implantation in pigs. These results are in line with previous reports on a macrophage-based foreign body response against gelatin-based hydrogel implants [57]. However, the decrease in macrophage accumulation within only 28 days after implantation may indicate a mild foreign body reaction against the implanted GelMA sealant. Further preclinical long-term studies could add information on the time course of macrophage response to GelMA implants as well as to the subtypes of macrophages involved in this process. Such a subtype classification may enable a differentiation between macrophage accumulation in terms of wound healing versus mild inflammatory response against the implants.

After 14 days in the pig defect model, the repaired defect site was still detectable, whereas GelMA was no longer present. Twenty-eight days after the sealing of a rat lung leakage, histology revealed substantial remodeling of the GelMA cover by invading host cells. These results proved sufficient wound repair within a short period of time. Besides adequate wound healing, biodegradation of the sealant seems to have happened, which might be achieved by host collagenases, i.e. primarily the matrix metalloproteinases 1, 8 and 13 [58]. Moreover, the matrix metalloproteinase 9, also known as gelatinase B, may play an important role for the biodegradation of the GelMA sealant, since it exerts a strong cleavage activity on gelatin [59]. Rapid *in vivo* degradation of gelatin-based biomaterials has been reported in previous studies [33,60,61], supporting the validity of our present observation that GelMA sealant underwent early degradation on rat and porcine lung lesions. Our *in vitro* degradation tests also revealed that the degradation kinetics of GelMA sealant were highly tunable, and that GelMA hydrogels with the optimized prepolymer concentrations degrade rapidly *in vitro*. Furthermore, it has been observed that the degradation of the GelMA hydrogels is dependent on the prepolymer concentration as well as the UV crosslinking time. This may explain why GelMA had disappeared from the lung defect site within 14 days after sealing, since the crosslinking time was only 0.5 min. However, 28 days after subcutaneous implantation of thicker GelMA samples, no macroscopically relevant degradation was observed. It may be hypothesized that the mechanical stresses on the lung and collagenase/gelatinase activity in the serous pleural fluid had contributed to faster degradation of GelMA in this position, or that the material remnants had simply detached after defect repair.

In terms of hemostasis, GelMA sealant was sufficient in stopping mild hemorrhage from the generated rat and porcine lung lesions. However, thorough investigation of the actual hemostatic potential of the sealant should be performed in adequate bleeding models, such as in a liver laceration model, which has been recently used to test the effect of shear-thinning nanocomposite hydrogels when applied in otherwise lethal hemorrhaging [36,41]. In this context, appropriate modification of GelMA sealant may allow for the creation of an effective sealant with strong hemostatic properties. Due to the fact that the pulmonary airways are a non-sterile environment, frequently evoking severe infections after lung surgery, antibacterial functionality may be another desirable property of a pulmonary sealant [62]. This feature may be provided by including silver or copper oxide nanoparticles or nanoparticle-carried antibiotic drugs within the sealant [63–65].

In the present study, we showed the successful application of our engineered sealant on lung lesion sites that are easily accessible. In real life scenarios, pulmonary defects may also occur in areas with restricted accessibility. In these cases, it should be possible to deliver the light for the crosslinking procedure by utilizing small light probes that can be also used in minimally invasive surgery to crosslink the applied biomaterials. Our future studies will focus on designing such light sources to extend the spectrum of applications of our engineered adhesive to minimally invasive surgery, and to also allow for the sealing of defects with difficult access. Moreover, we will examine different non-UV-bound photoinitiator systems for hydrogel crosslinking.

In our animal models, a small amount of GelMA prepolymer was applied on the defect sites. When using a larger amount of the material in real life scenarios, the high swelling potential of the material should be considered. In order to avoid local compression in restricted areas, only thin layers of GelMA hydrogel should be created, the sealing efficiency of which was shown in the present study.

5. Conclusions

Surgical glues are emerging biomedical tools that supplement conventional techniques like suturing or stapling, and have the strong potential to replace them. Besides general requirements, such as high biocompatibility, the broad variety of possible defect scenarios in different tissues demands adhesives with targeted properties.

The present study reports the suitability, effectiveness, and biocompatibility of a light-activated, gelatin-based hydrogel as a sealant for highly stressed elastic tissues. ASTM standard tests as well as chronic small and translational large animal models of lung leakage in the absence of prior sutures or staples proved GelMA sealant to exhibit excellent mechanical properties, including wound closure strength, shear resistance, and burst pressure, all of which outperformed clinical standard glues as well as sutures. Furthermore, GelMA sealant was shown to avoid a relevant inflammatory host response *in vivo* and to degrade quickly while allowing for adequate wound healing at the same time. Combining

our results with the low costs, ease of synthesis and application, and flexibility that minimizes adjacent tissue damage by avoiding mechanical compliance mismatch, GelMA sealant offers strong potential for commercialization as a sealant for air leakages.

The data of the present study suggests that large-scale testing of GelMA sealant in our translational large animal model should be the viable next step in establishing a new lung sealant.

Author contributions

AA, NA and AK designed the experiments. AV, MGR, SB, ESS and IN conducted the *in vitro* experiments. AA, AV, ESS, GUR and MGR conducted the small animal experiments. GC and SG conducted the large animal experiments. AA, AV, MGR, SB, IN, ESS, AK and NA analyzed the *in vitro* experiments. AA, AV, MGR, AT, AK and NA analyzed the small animal experiments. AA, GC, AK and NA analyzed the large animal experiments. AA wrote the manuscript. AK and NA provided major revisions. NA, AT and AK provided comments to the manuscript. All authors reviewed the manuscript.

Acknowledgements

The authors gratefully acknowledge Lay-Hong Ang for her work and support regarding histological and immunohistological readout, and Mina Keshvardoost for her work in the degradation experiments. AA acknowledges postdoctoral funding from the German Heart Foundation, Frankfurt, Germany. SB acknowledges funding from MIT-Italy program (Progetto Rocca) and Polimi International Fellowship (PIF). The authors acknowledge funding from the National Institutes of Health (AR057837, DE021468, D005865, AR068258, AR066193, EB022403, EB021148), and the Office of Naval Research Presidential Early Career Award for Scientists and Engineers (PECASE). N.A. acknowledges the support from the American Heart Association (AHA, 16SDG31280010), FY17 TIER 1 Interdisciplinary Research Seed Grants from Northeastern University, and the startup fund provided by the Department of Chemical Engineering, College of Engineering at Northeastern University.

Appendix A. Supplementary data

Supplementary data related to this article can be found at http://dx.doi.org/10.1016/j.biomaterials.2017.06.004.

References

[1] H. Itano, The optimal technique for combined application of fibrin sealant and bioabsorbable felt against alveolar air leakage, Eur. J. Cardiothorac. Surg. 33 (2008) 457–460.
[2] M. Glickman, A. Gheissari, S. Money, J. Martin, J.L. Ballard, C.M.V. Surger, A polymeric sealant inhibits anastomotic suture hole bleeding more rapidly than gelfoam/thrombin - results of a randomized controlled trial, Arch. Surg-Chicago 137 (2002) 326–331.
[3] N. Annabi, A. Tamayol, S.R. Shin, A.M. Ghaemmaghami, N.A. Peppas, A. Khademhosseini, Surgical materials: current challenges and nano-enabled solutions, Nano Today 9 (2014) 574–589.
[4] N. Annabi, K. Yue, A. Tamayol, A. Khademhosseini, Elastic sealants for surgical applications, Eur. J. Pharm. Biopharm. Off. J. ArbeitsgemeinschaftPharmazeutische Verfahrenstechnik eV 95 (2015) 27–39.
[5] S. Wolbank, V. Pichler, J.C. Ferguson, A. Meinl, M. van Griensven, A. Goppelt, et al., Non-invasive in vivo tracking of fibrin degradation by fluorescence imaging, J. Tissue Eng. Regen. Med. 9 (2015) 973–976.
[6] L. Montanaro, C.R. Arciola, E. Cenni, G. Ciapetti, F. Savioli, F. Filippini, et al., Cytotoxicity, blood compatibility and antimicrobial activity of two cyanoacrylate glues for surgical use, Biomaterials 22 (2000) 59–66.
[7] W.D. Spotnitz, S. Burks, Hemostats, sealants, and adhesives III: a new update as well as cost and regulatory considerations for components of the surgical toolbox, Transfusion 52 (2012) 2243–2255.
[8] F. Scognamiglio, A. Travan, I. Rustighi, P. Tarchi, S. Palmisano, E. Marsich, et al., Adhesive and sealant interfaces for general surgery applications, J. Biomed. Mater. Res. Part B Appl. Biomater. 104 (2016) 626–639.
[9] W.D. Spotnitz, S. Burks, Hemostats, sealants, and adhesives: components of the surgical toolbox, Transfusion 48 (2008) 1502–1516.
[10] R. Bitton, E. Josef, I. Shimshelashvili, K. Shapira, D. Seliktar, H. Bianco-Peled, Phloroglucinol-based biomimetic adhesives for medical applications, Acta Biomater. 5 (2009) 1582–1587.
[11] M. Mehdizadeh, H. Weng, D. Gyawali, L. Tang, J. Yang, Injectable citrate-based mussel-inspired tissue bioadhesives with high wet strength for sutureless wound closure, Biomaterials 33 (2012) 7972–7983.
[12] C. Ghobril, M.W. Grinstaff, The chemistry and engineering of polymeric hydrogel adhesives for wound closure: a tutorial, Chem. Soc. Rev. 44 (2015) 1820–1835.
[13] E.L. Park, J.B. Ulreich, K.M. Scott, N.P. Ullrich, J.A. Linehan, M.H. French, et al., Evaluation of polyethylene glycol based hydrogel for tissue sealing after laparoscopic partial nephrectomy in a porcine model, J. Urol. 172 (2004) 2446–2550.
[14] K.D. Than, C.J. Baird, A. Olivi, Polyethylene glycol hydrogel dural sealant may reduce incisional cerebrospinal fluid leak after posterior fossa surgery, Neurosurgery 63 (2008) 182–186.
[15] T.M. Shazly, N. Artzi, F. Boehning, E.R. Edelman, Viscoelastic adhesive mechanics of aldehyde-mediated soft tissue sealants, Biomaterials 29 (2008) 4584–4591.
[16] J.K. Tessmar, A.M. Gopferich, Customized PEG-derived copolymers for tissue-engineering applications, Macromol. Biosci. 7 (2007) 23–39.
[17] W.R. Ranger, D. Halpin, A.S. Sawhney, M. Lyman, J. Locicero, Pneumostasis of experimental air leaks with a new photopolymerized synthetic tissue sealant, Am. Surg. 63 (1997) 788–795.
[18] P. Macchiarini, J. Wain, S. Almy, P. Dartevelle, Experimental and clinical evaluation of a new synthetic, absorbable sealant to reduce air leaks in thoracic operations, J. Thorac. Cardiovasc. Surg. 117 (1999) 751–758.
[19] E. Buskens, M. Meijboom, H. Kooijman, B. Van Hout, The use of a surgical sealant (CoSeal®) in cardiac and vascular reconstructive surgery: an economic analysis, J. Cardiovasc. Surg. 47 (2006) 161.
[20] A. Belboul, L. Dernevik, O. Aljassim, B. Skrbic, G. Radberg, D. Roberts, The effect of autologous fibrin sealant (Vivostat) on morbidity after pulmonary lobectomy: a prospective randomised, blinded study, Eur. J. Cardiothorac. Surg. 26 (2004) 1187–1191.
[21] A. D'Andrilli, C. Andreetti, M. Ibrahim, A.M. Ciccone, F. Venuta, U. Mansmann, et al., A prospective randomized study to assess the efficacy of a surgical sealant to treat air leaks in lung surgery, Eur. J. Cardiothorac. Surg. 35 (2009) 20–21, 817-20; discussion.
[22] L. Bertolaccini, P. Lyberis, E. Manno, Lung sealant and morbidity after pleural decortication: a prospective randomized, blinded study, J. Cardiothorac. Surg. 5 (2010) 45.
[23] N. Lang, M.J. Pereira, Y. Lee, I. Friehs, N.V. Vasilyev, E.N. Feins, et al., A blood-resistant surgical glue for minimally invasive repair of vessels and heart defects, Sci. Transl. Med. 6 (2014) 218ra6.
[24] A. Brunelli, M. Monteverde, A. Borri, M. Salati, R.D. Marasco, A. Fianchini, Predictors of prolonged air leak after pulmonary lobectomy, Ann. Thorac. Surg. 77 (2004) 1205–1210 discussion 10.
[25] C.M. Elvin, T. Vuocolo, A.G. Brownlee, L. Sando, M.G. Huson, N.E. Liyou, et al., A highly elastic tissue sealant based on photopolymerised gelatin, Biomaterials 31 (2010) 8323–8331.
[26] C. Fuller, Reduction of intraoperative air leaks with Progel in pulmonary resection: a comprehensive review, J. Cardiothorac. Surg. 8 (2013) 90.
[27] H. Kobayashi, T. Sekine, T. Nakamura, Y. Shimizu, In vivo evaluation of a new sealant material on a rat lung air leak model, J. Biomed. Mater Res. 58 (2001) 658–665.
[28] J.W. Nichol, S.T. Koshy, H. Bae, C.M. Hwang, S. Yamanlar, A. Khademhosseini, Cell-laden microengineered gelatin methacrylate hydrogels, Biomaterials 31 (2010) 5536–5544.
[29] K. Yue, G. Trujillo-de Santiago, M.M. Alvarez, A. Tamayol, N. Annabi, A. Khademhosseini, Synthesis, properties, and biomedical applications of gelatin methacryloyl (GelMA) hydrogels, Biomaterials 73 (2015) 254–271.
[30] D. Loessner, C. Meinert, E. Kaemmerer, L.C. Martine, K. Yue, P.A. Levett, et al., Functionalization, preparation and use of cell-laden gelatin methacryloyl-based hydrogels as modular tissue culture platforms, Nat. Protoc. 11 (2016) 727–746.
[31] C. Cha, S.R. Shin, X. Gao, N. Annabi, M.R. Dokmeci, X.S. Tang, et al., Controlling mechanical properties of cell-laden hydrogels by covalent incorporation of graphene oxide, Small 10 (2014) 514–523.
[32] S.R. Shin, H. Bae, J.M. Cha, J.Y. Mun, Y.C. Chen, H. Tekin, et al., Carbon nanotube reinforced hybrid microgels as scaffold materials for cell encapsulation, ACS Nano 6 (2012) 362–372.
[33] J. Visser, D. Gawlitta, K.E. Benders, S.M. Toma, B. Pouran, P.R. van Weeren, et al., Endochondral bone formation in gelatin methacrylamide hydrogel with embedded cartilage-derived matrix particles, Biomaterials 37 (2015) 174–182.
[34] J. Hjortnaes, G. Camci-Unal, J.D. Hutcheson, S.M. Jung, F.J. Schoen, J. Kluin, et al., Directing valvular interstitial cell myofibroblast-like differentiation in a hybrid hydrogel platform, Adv. Healthc. Mater. 4 (2015) 121–130.
[35] M. Nikkhah, N. Eshak, P. Zorlutuna, N. Annabi, M. Castello, K. Kim, et al., Directed endothelial cell morphogenesis in micropatterned gelatin methacrylate hydrogels, Biomaterials 33 (2012) 9009–9018.
[36] A.K. Gaharwar, R.K. Avery, A. Assmann, A. Paul, G.H. McKinley,

A. Khademhosseini, et al., Shear-thinning nanocomposite hydrogels for the treatment of hemorrhage, ACS Nano 8 (2014) 9833–9842.
[37] N. Annabi, S.M. Mithieux, P. Zorlutuna, G. Camci-Unal, A.S. Weiss, A. Khademhosseini, Engineered cell-laden human protein-based elastomer, Biomaterials 34 (2013) 5496–5505.
[38] L. Zhou, G.X. Tan, Y. Tan, H. Wang, J.W. Liao, C.Y. Ning, Biomimetic mineralization of anionic gelatin hydrogels: effect of degree of methacrylation, Rsc Adv. 4 (2014) 21997–22008.
[39] T.C. Lai, J. Yu, W.B. Tsai, Gelatin methacrylate/carboxybetaine methacrylate hydrogels with tunable crosslinking for controlled drug release, J. Mater Chem. B 4 (2016) 2304–2313.
[40] T. Chen, R. Janjua, M.K. McDermott, S.L. Bernstein, S.M. Steidl, G.F. Payne, Gelatin-based biomimetic tissue adhesive. Potential for retinal reattachment, J. Biomed. Mater. Res. Part B, Appl. Biomater. 77 (2006) 416–422.
[41] Y.N. Zhang, R.K. Avery, Q. Vallmajo-Martin, A. Assmann, A. Vegh, A. Memic, et al., A highly elastic and rapidly crosslinkable elastin-like polypeptide-based hydrogel for biomedical applications, Adv. Funct. Mater. 25 (2015) 4814–4826.
[42] A. Assmann, K. Zwirnmann, F. Heidelberg, F. Schiffer, K. Horstkotter, H. Munakata, et al., The degeneration of biological cardiovascular prostheses under pro-calcific metabolic conditions in a small animal model, Biomaterials 35 (2014) 7416–7428.
[43] U. Anegg, J. Lindenmann, V. Matzi, J. Smolle, A. Maier, F. Smolle-Juttner, Efficiency of fleece-bound sealing (TachoSil) of air leaks in lung surgery: a prospective randomised trial, Eur. J. Cardiothorac. Surg. 31 (2007) 198–202.
[44] B. Qerimi, P. Baumann, J. Husing, H.P. Knaebel, H. Schumacher, Collagen hemostat significantly reduces time to hemostasis compared with cellulose: COBBANA, a single-center, randomized trial, Am. J. Surg. 205 (2013) 636–641.
[45] Y. Katagiri, S.A. Brew, K.C. Ingham, All six modules of the gelatin-binding domain of fibronectin are required for full affinity, J. Biol. Chem. 278 (2003) 11897–11902.
[46] Gorgieva S, Kokol V. Collagen-vs. Gelatine-based Biomaterials and Their Biocompatibility: Review and Perspectives.
[47] A.K. Lynn, I.V. Yannas, W. Bonfield, Antigenicity and immunogenicity of collagen, J. Biomed. Mater Res. B Appl. Biomater. 71 (2004) 343–354.
[48] A. Al-Mayah, J. Moseley, M. Velec, K.K. Brock, Sliding characteristic and material compressibility of human lung: parametric study and verification, Med. Phys. 36 (2009) 4625–4633.
[49] W. Carver, E.C. Goldsmith, Regulation of tissue fibrosis by the biomechanical environment, Biomed. Res. Int. 2013 (2013) 101979.
[50] B.L. Hartland, T.J. Newell, N. Damico, Alveolar recruitment maneuvers under general anesthesia: a systematic review of the literature, Respir. Care 60 (2015) 609–620.
[51] J. Ernsting, Aviation Medicine, 3 ed., Butterworth-Heinemann, Oxford, 1999, p. 703.
[52] M.S. Allen, D.E. Wood, R.W. Hawkinson, D.H. Harpole, R.J. McKenna, G.L. Walsh, et al., Prospective randomized study evaluating a biodegradable polymeric sealant for sealing intraoperative air leaks that occur during pulmonary resection, Ann. Thorac. Surg. 77 (2004) 1792–1801.
[53] C. Fan, J. Fu, W. Zhu, D.A. Wang, A mussel-inspired double-crosslinked tissue adhesive intended for internal medical use, Acta biomater. 33 (2016) 51–63.
[54] S. Kull, I. Martinelli, E. Briganti, P. Losi, D. Spiller, S. Tonlorenzi, et al., Glubran2 surgical glue: in vitro evaluation of adhesive and mechanical properties, J. Surg. Res. 157 (2009) e15–21.
[55] H. Zhang, L.P. Bre, T. Zhao, Y. Zheng, B. Newland, W. Wang, Mussel-inspired hyperbranched poly(amino ester) polymer as strong wet tissue adhesive, Biomaterials 35 (2014) 711–719.
[56] A.O. Elzoghby, Gelatin-based nanoparticles as drug and gene delivery systems: reviewing three decades of research, J. Control Release 172 (2013) 1075–1091.
[57] T. Yu, W. Wang, S. Nassiri, T. Kwan, C. Dang, W. Liu, et al., Temporal and spatial distribution of macrophage phenotype markers in the foreign body response to glutaraldehyde-crosslinked gelatin hydrogels, J. Biomater. Sci. Polym. Ed. 27 (2016) 721–742.
[58] M. Giannandrea, W.C. Parks, Diverse functions of matrix metalloproteinases during fibrosis, Dis. Model Mech. 7 (2014) 193–203.
[59] P.E. Van den Steen, B. Dubois, I. Nelissen, P.M. Rudd, R.A. Dwek, G. Opdenakker, Biochemistry and molecular biology of gelatinase B or matrix metalloproteinase-9 (MMP-9), Crit. Rev. Biochem. Mol. Biol. 37 (2002) 375–536.
[60] S.T. Koshy, T.C. Ferrante, S.A. Lewin, D.J. Mooney, Injectable, porous, and cell-responsive gelatin cryogels, Biomaterials 35 (2014) 2477–2487.
[61] J.Y. Lai, Y.T. Li, Functional assessment of cross-linked porous gelatin hydrogels for bioengineered cell sheet carriers, Biomacromolecules 11 (2010) 1387–1397.
[62] D.N. Nan, M. Fernandez-Ayala, C. Farinas-Alvarez, R. Mons, F.J. Ortega, J. Gonzalez-Macias, et al., Nosocomial infection after lung surgery: incidence and risk factors, Chest 128 (2005) 2647–2652.
[63] J.J. Buckley, P.L. Gai, A.F. Lee, L. Olivi, K. Wilson, Silver carbonate nanoparticles stabilised over alumina nanoneedles exhibiting potent antibacterial properties, Chem. Commun. (2008) 4013–4015.
[64] J. Deacon, S.M. Abdelghany, D.J. Quinn, D. Schmid, J. Megaw, R.F. Donnelly, et al., Antimicrobial efficacy of tobramycin polymeric nanoparticles for Pseudomonas aeruginosa infections in cystic fibrosis: formulation, characterisation and functionalisation with dornase alfa (DNase), J. Control Release 198 (2015) 55–61.
[65] M.S. Hassan, T. Amna, O.B. Yang, M.H. El-Newehy, S.S. Al-Deyab, M.S. Khil, Smart copper oxide nanocrystals: synthesis, characterization, electrochemical and potent antibacterial activity, Colloids Surf. B Biointerfaces 97 (2012) 201–206.